Tikrit Journal of Pure Science Vol. 30 (4) 2025

DOI: https://doi.org/10.25130/tjps.v30i4.1780

IRAQI Academic Scientific Journals

Tikrit Journal of Pure Science

ISSN: 1813 – 1662 (Print) --- E-ISSN: 2415 – 1726 (Online)

Journal Homepage: https://tjpsj.org/

Tikrit Journal of Pure Science

Structural Characterization and Electrical Properties of Barium Titanate Nanorod Crystals Synthesized via Hydrothermal Methods

Mubarak Hamad Oglah

Department of Mechanics Engineering, College Shirgat Engineering, Tikrit University, Tikrit, Iraq

Received: 28 Sep. 2024 **Received in revised forum:** 30 Nov. 2024 **Accepted:** 5 Dec. 2024

Final Proof Reading: 7 Aug. 2025 **Available online:** 25 Aug. 2025

ABSTRACT

Barium titanate nanorods (BTNRs) were formed via the hydrothermal process through preliminary preparation of a slurry of hydroxide precursors by mixing $BaCl_2.H_2O$ and $TiCl_2$ with a (10 Molar) of NaOH solution. The hydroxide slurry was heated at (205 °C) for (24 h) to complete the process. This study focused on examining the electrical properties of nanoscale barium titanate ($BaTiO_3$) synthesized via the hydrothermal technique. Scanning Electron Microscopy (SEM) imaging demonstrated the unique rod-like shape of barium titanate nanorods, confirming their production. Furthermore, X-ray diffraction (XRD) analysis confirmed the crystalline structure attained under the experimental circumstances and confirmed the successful production of the $BaTiO_3$ perovskite phase. Fourier Transform Infrared Spectroscopy (FTIR) was utilized to identify the functional groups present in the nanomaterial. Additionally, the structure and composition of $BaTiO_3$ were confirmed using Energy Dispersive Spectroscopy (designed as EDS). The electrical conductivity was assessed utilizing the four-point probe (4-point electrical conductivity) method to determine sheet resistance, while impedance spectroscopy was used to investigate the capacitance, and dielectric constant. The results revealed the intrinsic properties of $BaTiO_3$ nanorods, highlighting its potential applications in electronics and capacitors.

Keywords: Hydroxide precursor, Hydrothermal, Barium titanate, Piezoelectric, Electrical properties.

Name: **Mubarak Hamad Oglah** **E-mail:** **mubarak@tu.edu.iq**

Tikrit Journal of Pure Science Vol. 30 (4) 2025
DOI: https://doi.org/10.25130/tjps.v30i4.1780

التوصيف التركيبي والخصائص الكهربائية لبلورات تيتانات الباريوم النانوية المحضرة باستخدام الطريقة المائية الحرارية

مبارك حمد عكلة

قسم الهندسة الميكانيكية، كلية هندسة الشرقاط، جامعة تكريت، العراق

الملخص

تم تشكيل قضبان نانوية من تيتانات الباريوم (BTNRs) من خلال العملية الحرارية المائية ومن خلال التحضير الأولي لمزيج من سلائف الهيدروكسيد عن طريق خلط $BaCl_2.H_2O$ و $TiCl_2$ مع 10 مولار من محلول NaOH. تم تسخين مزيج الهيدروكسيد عند (205 ^oC) لمدة 24 ساعة لإكمال العملية. ركزت هذه الدراسة على تشخيص الخصائص الكهربائية لتيتانات الباريوم النانوية ($BaTiO_3$) المصنعة عبر التقنية الحرارية المائية. كشفت صور المجهر الإلكتروني الماسح عن مؤشر قوي على بنية القضيب النانوي، بينما تم إجراء فحص حيود الأشعة السينية (XRD) لتأكيد البنية البلورية وتحديد الطور البلوري للمادة، وتم استخدام مطيافية تحويل فوريه بالأشعة تحت الحمراء (FTIR) لتحديد المجموعات الوظيفية الموجودة في المادة النانوية. بالإضافة إلى ذلك، تم تأكيد بنية وتركيب $BaTiO_3$ باستخدام مطيافية تشتت الطاقة (المصممة كـ EDS). تم تقييم الموصلية الكهربائية باستخدام طريقة المسبار ذي النقاط الأربع (الموصلية الكهربائية ذات النقاط الأربع) لتحديد مقاومة الصفيحة، في حين تم استخدام مطيافية الممانعة الكهربائية للتحقيق في السعة وثابت العازل. كشفت النتائج عن الخصائص الجوهرية لقضبان $BaTiO_3$ النانوية، وسلطت الضوء على تطبيقاتها المحتملة في الإلكترونيات والمكثفات.

INTRODUCTION

Barium Titanate ($BaTiO_3$) is broadly utilized in capacitors, sensors and actuators because of the fact that it is a known ferroelectric ceramic material possessing the perovskite structure[1]. $BaTiO_3$ exhibits significant dielectric, piezoelectric, and ferroelectric properties, which are crucial for various electronic applications. Piezoelectric nanomaterials can alter electrical voltage into mechanical force and vice versa, making them perfect for utilize in actuators and sensors [1]. This research aims to determine the electrical properties of nanostructured $BaTiO_3$ synthesized via the hydrothermal method, a technique known for producing high-purity and crystalline materials.

Inclusive research on the hydrothermal preparation of nanomaterials, exploring various techniques and applications, such as energy harvesting and biosensing. Their research highlighted the advantages of hydrothermal methods, including the ability to produce stable nanomaterials under varying temperature and pressure conditions [2]. Barium titanate has unique properties because of its perovskite crystal structure [3-6]. In a study by [7] it was discovered the possibility of obtaining $BaTiO_3$ nanorods as a result of treating a single-stage solubility precipitation mechanism with ethylene glycol, using it as a stabilizing medium. Consequently, their synthesis is accompanied with formation of uniform crystals-in particular single uniform crystals. These nanorods have tetragonal structure with c-axis/a-axis ratio equal to (1.0111), whereas $BaTiO_3$ particles synthesized in the absence of ethylene glycol looked like cubes. Previous research has shown that the hydroxyl groups (OH) in ethylene glycol (EG) play a crucial role in stabilizing the tetragonal structure [8, 9]. It has been observed that nanostructured $BaTiO_3$ materials show better properties because surface atoms

contribute more and there may be different physical laws that do not exist in bulk matter. For instance, the synthesis of $BaTiO_3$ nanowires, nanoplates, and nanorods has opened novel paths for the strategy of high-performance actuators, energy storage devices and sensors. The emergence of nanostructures (nanowires, Nano platelets, and nanotubes) suggests a potential paradigm shift in nanocomposites. Recent studies have indicated that composites reinforced with nanorods or nanowires possess higher dielectric permittivity and tensile strength when compared to composites reinforced with nanoparticles [10-12]. The influence of nanostructures ceramic on the piezoelectric properties of BaTiO3 was investigated. By employing normal sintering methods and spark plasma sintering (SPS), the researchers demonstrated that smaller ferroelectric domain sizes significantly enhanced the piezoelectric constant, achieving a high piezoelectric coefficient (d33) of 416 pC/N in nanoceramics with domains less than 50 nm in width ([13]. Explored the applications of the BT-101 dielectric material in improving the performance of electroluminescent (EL) lamps by [14]. In this study, aim to synthesize barium titanate BaTiO3 nanoparticles by hydrothermal method, and analyze their structural and electrical properties comprehensively, focusing on the electrical properties. In addition, the structure of the synthesized nanorod will be examined, characterize the crystal structure of the sample and identify the functional groups in it.

2- EXPERIMENTAL

Preparation of Barium Titanate Nanorods

Barium titanate nanorods (BTNRs) were formed by a precipitation-aging technique including a precursor slurry, followed by a hydrothermal process. The (Ba-Ti-OH) precursor was prepared using barium chloride ($BaCl_2$, Kishida Chemical.), Titanium tetrachloride ($TiCl_4$ solution (Sigma-Aldrich) and Hydroxide Sodium (NaOH, Nacalai Tesque (98 %)). A mixture of (1 M) $BaCl_2$ (20 ml aqueous solution) and (0.6 M) $TiCl_4$ solution (10 ml aqueous. solution) was prepared at (25 °C) temperature, then adding (10 %) NaOH to this slurry as a solvent and (35 ml) of deionized (DI) water. The hydrothermal process was adjusted the over-all size of the precursor slurry to (80 ml). Consequently, the precursor slurry was heated using a teflon-lined autoclave (150 ml vessel). The hydroxide slurry was heated at (205 °C) for (24 h) to complete the process. Following hydrothermal process, the product was detached by centrifuge device, and then washed several times by DI water, and dried at (80 °C), (see figure 1).

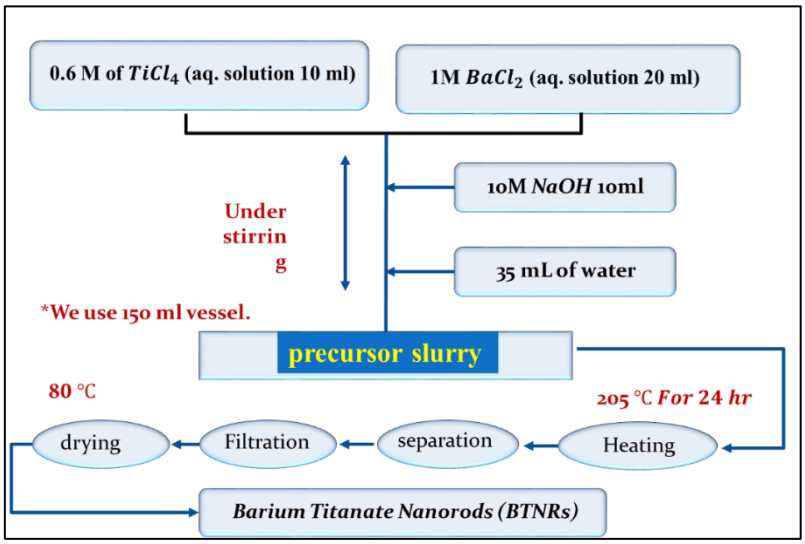

Fig.1: Illustrative diagram of the stages of $BaTiO_3$ nanorods preparation by using the hydrothermal method.

Characterization of Barium Titanate Nanorods

SEM images was conducted to investigate morphology of barium titanate nanorods (using an Axia Chemi at an applied voltage of 5kV). XRD patterns (PA-analytical, X-Pert PRO MPD, using Cu-K radiation at 30 KV) was employed to govern the crystalline structure and phase of the manufactured $BaTiO_3$. The diffraction patterns were analyzed to confirm the $BaTiO_3$ crystalline structure. EDS analysis was conducted to investigate the elemental compound of the synthesized $BaTiO_3$ nanoparticles. FTIR spectroscopy was used to detect the functional-groups and chemical bonds in the $BaTiO_3$ nanorods, providing insights into the molecular structure. The FTIR spectra were captured through the attenuated total reflectance (ATR) method used (a Zn-Se crystal) within the Nicolet IS50 spectrometer (Thermo Fisher, USA), spanning a range of (4500–0 cm^{-1}). The four-point probe technique was utilized to measure the sheet resistance and electrical conductivity of the $BaTiO_3$ nanoparticles. This method provides accurate resistivity measurements by minimizing contact resistance effects. The measurement data for barium titanate using the 4-point probe method indicate a significant difference in voltage readings between channels. The sheet resistance (ρ_s) is determined using the 4-point probe method, as described by the equation (1) [15],

$$\rho_s = \frac{V}{I} 4.5324\ [\Omega.sq] \qquad (1)$$

Where, I is the current through the outer probes (nA), and V is the voltage between the inner probes (mV). The impedance spectroscopy was used to study capacitance, permittivity and dielectric constant. The primary aim is to determine the relative permittivity ($\varepsilon^{`}$) and electrical conductivity (σ) of the material based on the measured impedance data at various frequencies. Hence, Radius of the disk (r) is (0.01 m) and Thickness of the sample (d) was (1 mm), Vacuum permittivity (ε_o) is (8.858×10^{-12} f/m).

RESULTS AND DISCUSSION

Characterization of Barium Titanate Nanorods

FTIR spectra was conducted to detect functional groups within the powder sample, as depicted in Figure 2(a). The resulting FTIR absorbance spectra was recorded in transmittance mode over the range of (4500–0 cm^{-1}). The functional group of (Ti-O) band is at (562 cm^{-1}) is indicative of the barium titanate structure and is influenced by Ba ions. The functional group of (Ba-Ti-O) bonds appear in the (1430–1630 cm^{-1}) range, whereas the C-O bands at (1110 cm^{-1}) suggest the presence of residual ethylene glycol (EG) or potential C-C stretching. The C–H band is at (2877 cm^{-1}), representing the connecting of ethylene glycol groups to titanium. The absence of Ba-C-O intensity in the $BaTiO_3$ powder suggests a reduced formation of $BaCO_3$. The OH-OH groups are observable in the (3425 cm^{-1}) band. The peroxide synthesis of surface-functionalized barium titanate nanoceramic is revealed by the presence of hydroxyl groups on the (OH) surface functional group. It is interesting that there are some spectra with very low transmittance ranges, which are referred to the changing chemical reactions, nature of materials, and crystallization of compounds at higher temperatures and are not considered [1, 16]. Figure 2(b) presents XRD pattern of the $BaTiO_3$ nanorods (BTNRs). The XRD analysis, consistent with (JCPDS no. #892475), reveals the creation of a structure nanorods phase characterized by a lattice parameter of (a = 4.0217 Å). The most intense peak (110) is observed at (2θ = 32.17°). Additional peaks detected at (2θ = 22.208° (100), 32.17° (110), 38.898° (111), 45.590° (200), 50.812° (210), 56.127° (211), 65.779° (220), 70.323° (300), and 74.788° (310)), further authorize the formation of structure perovskite of $BaTiO_3$ as in [17, 18]. Minor peaks are ascribed to the formation of $BaCO_3$, resulting from the interaction of barium hydroxide with CO_2 released during the annealing process. The smallest crystallite size of the barium titanate nanopowder, estimated utilizing the Debye-

Scherrer equation considering peak broadening, was (11 nm). The mean crystallite size, derived from multiple peaks, was determined to be (78 nm), the Scherrer formula given as equation (2) [19]:

$$D = \frac{k\lambda}{\beta cos\theta} \quad (2)$$

where θ is the Bragg's angle D is crystallite size of domains, k is shape factor, and its value is(0.91), λ is the wavelength of X-rays, and β is full width at half maxima (FWHM) in radians.

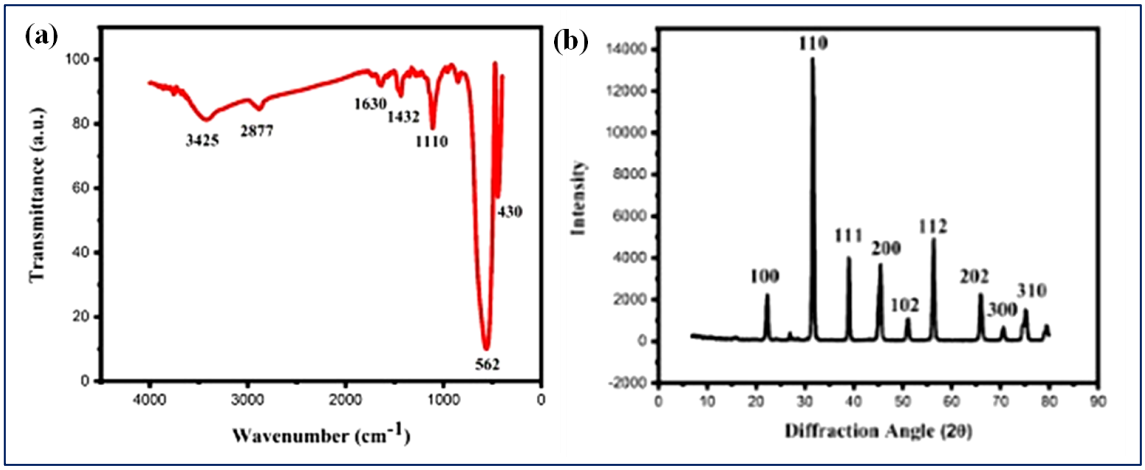

Fig. 2: (a) FTIR spectrum of $BaTiO_3$, (b) XRD patterns a tetragonal $BaTiO_3$ nanostructure

Figure 3 illustrated SEM images of the prepared samples showed clear patterns of barium titanate nanorods. It can be seen that the overall shape of the particles ranges from rods to microplates. Furthermore, small agglomerates of nanorods can be observed, indicating some agglomeration during the preparation process. The dispersion of the particles appears to be good, indicating a relatively homogeneous distribution of particles within the sample. The surface of the nanorods appears generally smooth, with some rough appearances that may be caused by the crystallization process during preparation. The high temperature (205 °C) and long reaction time (24 h) contributed to the formation of nanorods with the specified shape and size. These conditions promote crystallization and longitudinal growth of the rods [20]. The observed agglomerations may be a result of surface interactions between nanorods during the preparation process. These agglomerations are likely the result of van der waals attractive forces or hydrogen bonding between molecules. The nanoscale shape and small dimensions of nanorods may give these materials distinct physical and chemical properties such as improved electrical insulation and increased catalytic activity in various applications.

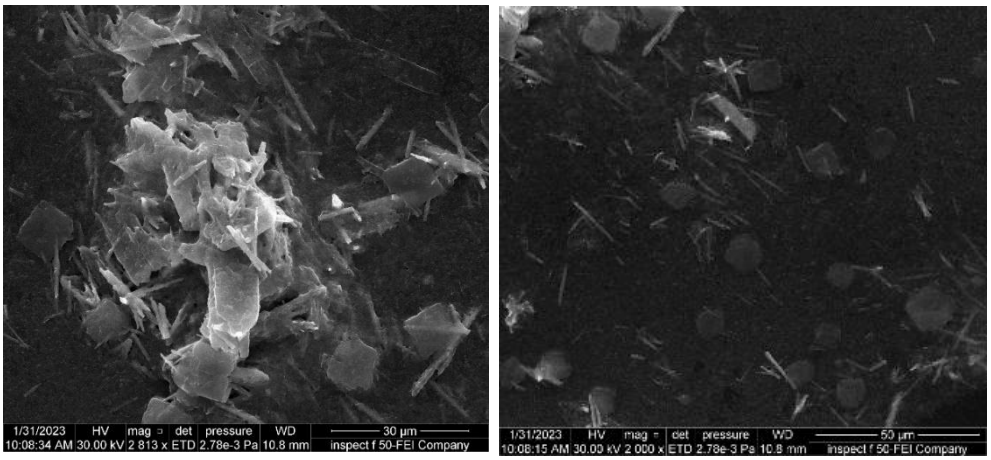

Fig. 3: SEM images of the hydrothermal products synthesized at 205 °C for 20 h, displayed at various magnifications.

Table 1 illustrated, oxygen appears weight percentage (28.30 %) and atomic percentage: (67.50 %) as a significant proportion in the composition, indicating oxide formation in the sample. Titanium is a major component of nanorods, supporting the formation of barium titanate and exhibits weight percentage (24.23 %) and Atomic percentage (19.31 %). The high percentage of barium (Ba) indicates a major role for this element in the general structure of nanorods (47.47 % weight percentage). From the table, it is clear that barium titanate nanorods contain a large percentage of oxygen, titanium, and barium. The high oxygen content is in line with expectations because barium titanate is an oxide compound. The atomic percentage of oxygen (67.50 %) is very high compared to others, reflecting an oxide formation. The weight percentage of barium is the highest (47.47%), which enhances its prominent role in the synthesis of nanorods.

Table 1: Elements content of the samples determined by EDS (at. %)

Element	Line Type	Apparent Concentration	k Ratio	Wt.%	Wt.% Sigma	Atomic %
O	K series	9.71	0.03266	28.30	0.40	67.50
Ti	K series	7.10	0.07095	24.23	0.38	19.31
Ba	L series	12.30	0.11515	47.47	0.51	13.19
Total:				100.00		100.00

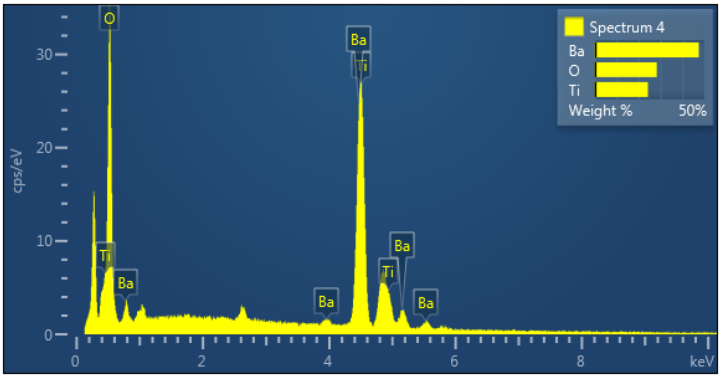

Fig. 4: Elements content of the samples determined by EDS (at. %)

Electrical Properties

The measurement data for barium titanate using the 4-point probe method indicate a significant difference in voltage readings between channels (see equation (3)) [21]. For Channel 2, the maximum voltage was (7400 mV), the minimum was (-9200 mV), resulting in a peak-to-peak voltage (Vpp) of (16600 mV), with an applied current of (3531.915 nA). Channel 1 showed a maximum voltage of (420 mV), a minimum of (-400 mV), and a Vpp of (820 mV) (see figure 4). The sheet resistance (ρ_s) is determined using the 4-point probe method, as described by the equation (3):

$$\rho_s = \frac{V}{I}\ 4.5324\ [ohms\ per\ square(\Omega.sq)] \quad (3)$$

Given: applied voltage (V = 16600 mV = 16.6 V) assuming peak-to-peak voltage is used and applied current (I = 3531.915 nA = 3.531915 μA)

$$\rho_s = \frac{16.6}{3.531915\times10^{-6}} \times 4.5324 = 1052281.301\ [\Omega.cm] \quad (4)$$

The calculated sheet resistance was (1052281.301 Ω.cm) which aligns with the high resistivity expected of barium titanate. The high sheet resistance value indicates that $BaTiO_3$ sample used here is highly resistive or insulating. This high resistance of the sheets emphasizes the dielectric properties of the material, which is known to be a ceramic material with high dielectric constant, making it suitable for electronic applications such as capacitors and piezoelectric devices. The four-point probe method is sensitive to several factors such as probe spacing and sample thickness resulting in inconsistency between channel readings.

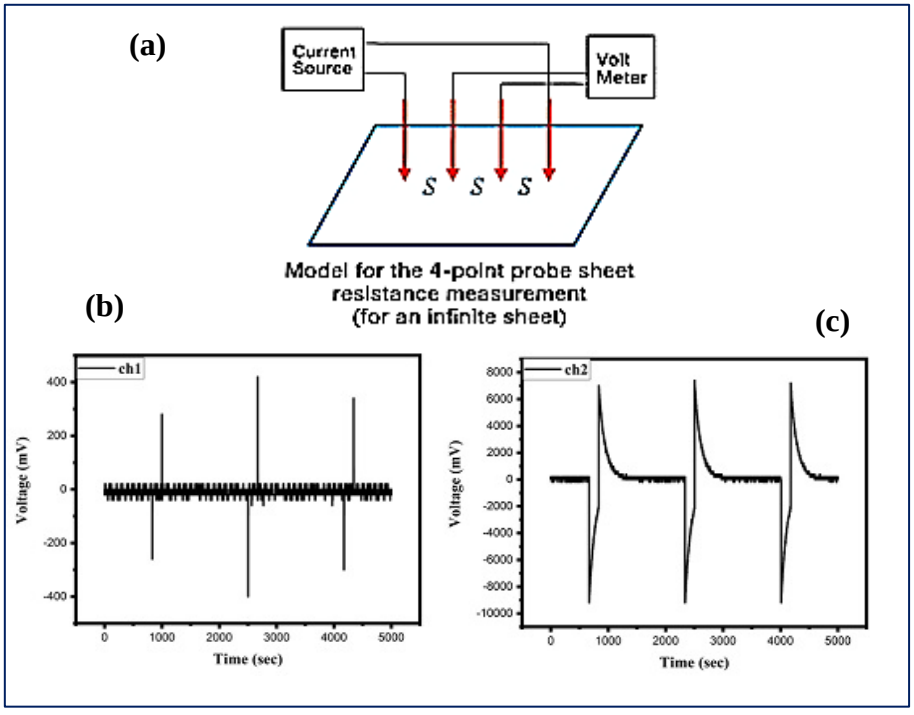

Fig. 5: (a) Measurement principle of the 4-point sheet resistance model, (b) Voltage of Channel 1 (Ch1), (c) Voltage of Channel 2 (Ch2).

The impedance data includes the real part (Z′) and the imaginary part (Z″) at different frequencies (f) (see figure 6(a). The horizontal axis (Z') represents the real part of impedance in (Ω.cm²), while the vertical axis (Z") represents the imaginary part of impedance in (Ω.cm²). The results show a gradually decreasing behavior of the curve, where the imaginary impedance decreases as the real impedance increases. Specifically, the real impedance (Z') increases from (0 to 100,000 Ω.cm²), while the imaginary impedance (Z") decreases to negative values reaching (-500,000 Ω.cm²). This behavior reflects the properties of dielectric materials such as barium titanate

nanorods. The observed decrease in imaginary impedance with increasing real impedance may indicate a charging and discharging process in the dielectric materials, suggesting an interaction between electrons and voids within the nanostructure of the material. The figure 6 (b) shows the variation of the dielectric constant of barium titanate with frequency. The dielectric constant was calculated by using the following relationship derived from imaginary impedance [22]:

$$C = \frac{1}{2\pi f|Z''|} \quad (5)$$

Where, (C) is Capacitance and f is frequency, or used Complex impedance ($Z^* = Z' + jZ''$)

Then, we found dielectric constant by using the following formula [23]:

$$\varepsilon' = \frac{C.d}{\varepsilon^o.A} \quad (6)$$

Hence, C is the capacitance, d is the thickness of the dielectric material, A is area ($A = \pi r^2$), d is the thickness of the sample, and ε^o is the permittivity of free space (8.854×10^{-12} F/m). It can be seen that the dielectric constant is high at low frequencies and then decreases significantly with increasing frequency until it reaches a quasi-stable value. At higher frequencies, we observe a sharp increase in the dielectric constant, indicating a phenomenon known as resonant frequencies [24, 25]. It can be seen that the amplitude is very high at low frequencies and then decreases sharply as the frequency increases. The amplitude continues to decrease until it reaches an almost constant value at high frequencies. This change reflects the contractile ability of the material to store electrical charge with increasing frequency. The capacitance value decrease with increasing frequency. This behavior is attributed to the material's ability to respond to rapidly changing electric fields. At high frequencies, it is difficult for the electric dipoles in the material to track rapid changes in the electric field, resulting in a decrease in capacitors, as show in figure 6(c). The decrease in capacitance with higher frequency indicates the material's limitations in applications that require a fast frequency response [26]. The sharp increase in the dielectric constant at high frequencies can be explained by the presence of resonant frequencies. These frequencies occur when the external frequency matches the natural frequency of the material, resulting in a significant increase in the dielectric constant [27-29]. The results indicate that nanoscale barium titanate possesses excellent dielectric properties at medium and high frequencies, making it suitable for use in energy storage applications and dielectrics in microelectronics.

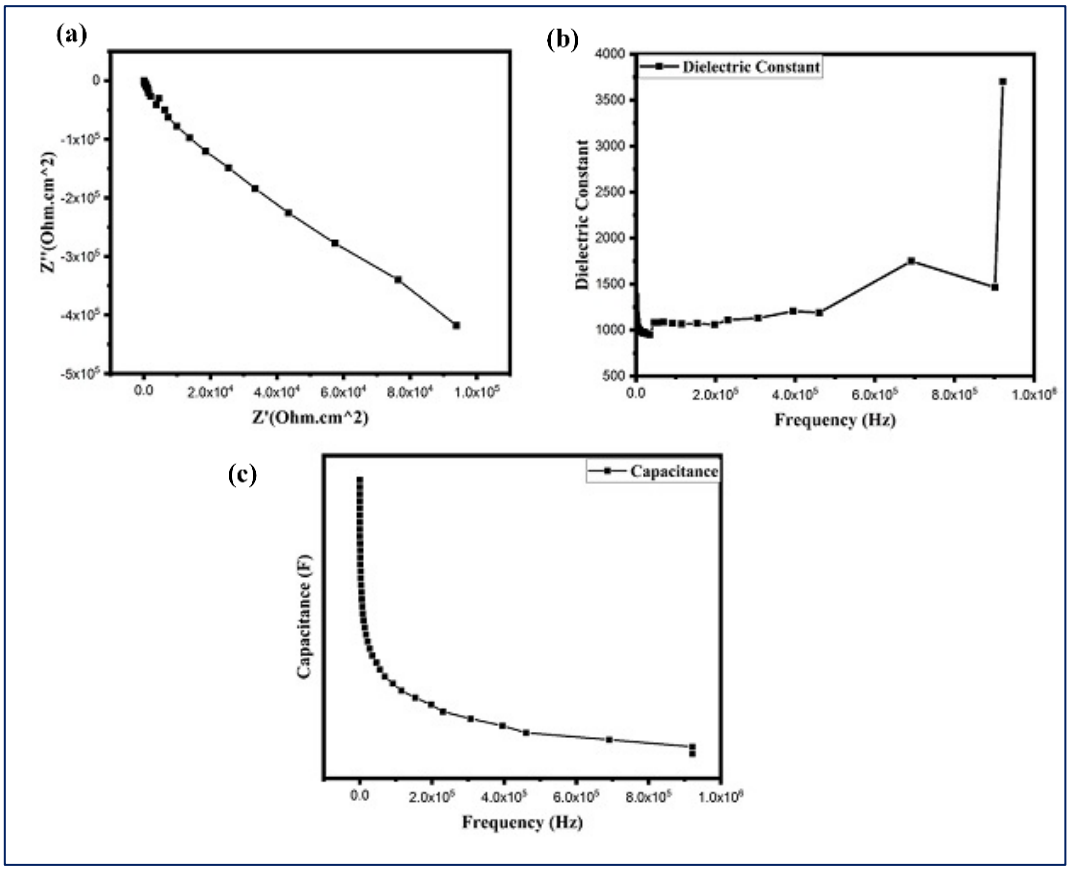

Fig. 6: Impedance spectroscopy of barium titanate powder at different frequencies, (b) Dielectric Constant vs. Frequency for barium titanate Nano powder, (c) The Capacitance vs. frequencies for BT nanorod

CONCLUSION

This study successfully synthesized nanostructured $BaTiO_3$ using the hydrothermal method and comprehensively analyzed its structural and electrical properties. The XRD, FTIR, and EDS results confirmed the high purity and crystalline nature of the material. The significant piezoelectric coefficient and electrical conductivity underscore the potential of $BaTiO_3$ nanorods in various electronic devices. Future work could explore the optimization of synthesis parameters to further enhance these properties and expand the application range of $BaTiO_3$ nanomaterials. The correlation between the structural characteristics and electrical properties of $BaTiO_3$ nanofillers demonstrates that the hydrothermal synthesis method produces high-quality nanomaterials with excellent electrical performance. The crystalline structure and purity directly influence the piezoelectric and conductive behaviors, making hydrothermally synthesized $BaTiO_3$ suitable for advanced various technical fields. The results came from dielectric, insulating, and resistance spectroscopy behavior indicate the possibilities of using barium titanate nanorods in electronic applications.

Conflict of interests: The authors declared no conflicting interests.

Sources of funding: This research did not receive any specific grant from funding agencies in the public, commercial, or not-for-profit sectors.

Author contribution: Authors contributed equally in the study.

REFERENCES

1. Kovalenko O, Škapin S, Kržmanc MM, Vengust D, Spreitzer M, Kutnjak Z, et al. Formation of single-crystalline BaTiO3 nanorods from glycolate by tuning the supersaturation conditions. Ceramics International. 2022;48(9):11988-97.

https://doi.org/10.1016/j.ceramint,2022,01.048

2. Jayatissa YXGAH, Yu Z, Chen X, Li M. Hydrothermal synthesis of nanomaterials. Journal of Nanomaterials. 2020;2019:NA-NA. https://doi.org/10.1155/2020/8917013

3. Mehmood MF, Habib A. Hydrothermal Synthesis and Structural Characterization of BaTiO3 Powder. The Nucleus. 2023;60(2):168-73.

4. Padalia D, Kumar U, Bhandari P, Dalal J, Ranakoti L, Singh T. Tuning the structural, optical, and dielectric properties of europium-doped barium titanate ceramics. Journal of Materials Science: Materials in Electronics. 2024;35(19):1375. https://doi.org/10.1007/s10854-024-12984-9

5. Pang X, Wang T, Liu B, Fan X, Liu X, Shen J, et al. Effect of solvents on the morphology and structure of barium titanate synthesized by a one-step hydrothermal method. International Journal of Minerals, Metallurgy and Materials. 2023;30(7):1407-16. https://doi.org/10.1007/s12613-023-2614-9.

6. Tewatia K, Sharma A, Sharma M, Kumar A. Factors affecting morphological and electrical properties of Barium Titanate: A brief review. Materials Today: Proceedings. 2021;44:4548-56. https://doi.org/10.1016/j.matpr.2020.10.813

7. Inada M, Enomoto N, Hayashi K, Hojo J, Komarneni S. Facile synthesis of nanorods of tetragonal barium titanate using ethylene glycol. Ceramics International. 2015;41(4):5581-7. https://doi.org/10.1016/j.ceramint.2014.12.137

8. Jian G, Jiao Y, Meng Q, Cao Y, Zhou Z, Moon K-S, et al. Hydrothermal synthesis of BaTiO 3 nanowires for high energy density nanocomposite capacitors. Journal of Materials Science. 2020;55:6903-14. https://doi.org/10.1007/s10853-020-04520-x

9. Yan Y, Xia H, Fu Y, Xu Z, Ni Q-Q. Controlled hydrothermal synthesis of different sizes of BaTiO3 nano-particles for microwave absorption. Materials Research Express. 2020;6(12):1250i3. https://doi.org/10.1088/2053-1591/ab6daf

10. Atallah FS, Ahmed HH, Jasim WK. Effect of Mg Molar Concentration on Structural and Optical Properties of CdO Thin Films Prepared by Chemical Bath Deposition Method. Tikrit Journal of Pure Science. 2020;25(3):103-9. https://doi.org/10.25130/tjps.v25i3.256

11. Baji A, Mai Y-W, Lin T. Effect of barium titanate reinforcement on tensile strength and dielectric response of electrospun polyvinylidene fluoride fibers. Novel Aspects of Nanofibers: IntechOpen London, UK; 2018. https://doi.org/10.5772/intechopen.74662

12. Mohammed SA, Ahmed AR, Ibrahim IM. High Performance of ZnO/PANI Nanocomposites for Supercapacitors Applications. Tikrit Journal of Pure Science. 2023;28(4):132-8. https://doi.org/10.25130/tjps.v28i4.1307

13. Shen Z-Y, Li J-F. Enhancement of piezoelectric constant d33 in BaTiO3 ceramics due to nano-domain structure. Journal of the Ceramic Society of Japan. 2010;118(1382):940-3. https://doi.org/10.2109/jcersj2.118.940

14. KIKKEN S, Vandalon V. Measuring film resistivity: understanding and refining the four-point probe set-up: B. Sc Thesis at the Department of Applied Physics Plasma & Materials; 2018.

15. Jiang B, Iocozzia J, Zhao L, Zhang H, Harn Y-W, Chen Y, et al. Barium titanate at the nanoscale: controlled synthesis and dielectric and ferroelectric properties. Chemical Society Reviews. 2019;48(4):1194-228. https://doi.org/10.1039/C8CS0058 3D

16. Liu Y, Chen T, Zheng J, Zhu Z, Huang Z, Hu C, et al. Enhanced piezo-catalytic performance of BaTiO3 nanorods combining highly exposed active crystalline facets and superior deformation capability: Water purification and activation mechanism. Chemical Engineering Journal. 2024;488:150768. https://doi.org/10.1016/j.cej.2024.150768.

17. Singh M, Yadav B, Ranjan A, Kaur M, Gupta S. Synthesis and characterization of perovskite barium

titanate thin film and its application as LPG sensor. Sensors and actuators b: chemical. 2017;241:1170-8. https://doi.org/10.1016/j.snb.2016.10.018

18. Žagar K, Rečnik A, Šturm S, Gajović A, Čeh M. Structural and chemical characterization of BaTiO3 nanorods. Materials research bulletin. 2011;46(3):366-71. https://doi.org/10.1016/j.materresbull.2010.12.012

19. Salem MM, Darwish MA, Altarawneh AM, Alibwaini YA, Ghazy R, Hemeda OM, et al. Investigation of the structure and dielectric properties of doped barium titanates. RSC advances. 2024;14(5):3335-45. https://doi.org/10.1039/D3RA05885A

20. Huang L, Liu T, Zhang H, Guo W, Zeng W. Hydrothermal synthesis of different TiO 2 nanostructures: Structure, growth and gas sensor properties. Journal of Materials Science: Materials in Electronics. 2012;23:2024-9. 10.1007/s10854-012-0697-6

21. Hue ĐTM, Kurisu M, Konishi K, Cong BT. STRUCTURE, ELECTRICAL PROPERTIES, AND APPLICATION POSIBILITY AS SOLID OXIDE FUEL CELLS CATHODE MATERIALS OF (La2NiO4±δ)(BaTiO3) x (x= 0.0-0.5) COMPOSITES. Journal of Science and Technology. 2016;54(1A):66-71. https://doi.org/10.15625/2525-2518/54/1A/11807

22. Ahmad SI, Rauf A, Mohammed T, Bahafi A, Kumar DR, Suresh MB. Dielectric, impedance, AC conductivity and low-temperature magnetic studies of Ce and Sm co-substituted nanocrystalline cobalt ferrite. Journal of Magnetism and Magnetic Materials. 2019;492:165666. 10.1016/j.jmmm.2019.165666

23.Nayak S, Sahoo B, Chaki TK, Khastgir D. Facile preparation of uniform barium titanate ($BaTiO_3$) multipods with high permittivity: impedance and temperature dependent dielectric behavior. 2013. https://doi.org/10.1039/C3RA44815K

24. He F, Ren W, Liang G, Shi P, Wu X, Chen X. Structure and dielectric properties of barium titanate thin films for capacitor applications. Ceramics International. 2013;39:S481-S5. https://doi.org/10.1016/j.ceramint.2012.10.118

25. Sandi D, Supriyanto A, Iriani Y, editors. The effects of sintering temperature on dielectric constant of Barium Titanate (BaTiO3). IOP Conference Series: Materials Science and Engineering; 2016: IOP Publishing. https://doi.org/10.1088/1757-899X/107/1/012069

26. Liu W, Lu C, Li H, Tay RY, Sun L, Wang X, et al. based all-solid-state flexible micro-supercapacitors with ultra-high rate and rapid frequency response capabilities. Journal of Materials Chemistry A. 2016;4(10):3754-64. https://doi.org/10.1039/C6TA00159A

27. Bolivar PH, Brucherseifer M, Rivas JG, Gonzalo R, Ederra I, Reynolds AL, et al. Measurement of the dielectric constant and loss tangent of high dielectric-constant materials at terahertz frequencies. IEEE Transactions on Microwave Theory and Techniques. 2003;51(4):1062-6. https://doi.org/10.1109/TMTT.2003.809693

28. Hussain AA, Abdullah QN. Studying the Structural, Optical and Electrical Properties of ZnO: SnO2 Thin Films as an Application of a Gas Sensor Using Vacuum Thermal Evaporation Technique. Tikrit Journal of Pure Science. 2023;28(6):66-75. https://doi.org/10.25130/tjps.v28i6.1379

29. Mongia RK, Bhartia P. Dielectric resonator antennas—A review and general design relations for resonant frequency and bandwidth. International Journal of Microwave and Millimeter-Wave Computer-Aided Engineering. 1994;4(3):230-47. https://doi.org/10.1002/mmce.4570040304